Aromatic C−H Activation and Catalytic Hydrophenylation of Ethylene by TpRu{P(OCH$_2$)$_3$CEt}(NCMe)Ph

Nicholas A. Foley,[†] Zhuofeng Ke,[§,⊥] T. Brent Gunnoe,*[,†] Thomas R. Cundari,*[,§] and Jeffrey L. Petersen[‡]

Department of Chemistry, North Carolina State University, Raleigh, North Carolina 27695-8204, C. Eugene Bennett Department of Chemistry, West Virginia University, Morgantown, West Virginia 26506-6045, Center for Advanced Scientific Computing and Modeling (CASCaM), Department of Chemistry, University of North Texas, Box 305070, Denton, Texas 76203-5070, and School of Chemistry & Chemical Engineering, Sun Yat-sen University, Guangzhou 510275, People's Republic of China

Received March 28, 2008

The complexes TpRu{P(OCH$_2$)$_3$CEt}(L)R {L = PPh$_3$ or NCMe; R = Cl, OTf (OTf = trifluoromethanesulfonate), or Ph; Tp = hydridotris(pyrazolyl)borate} and TpRu{P(OCH$_2$)$_3$CEt}(η^3-C$_3$H$_4$Me) were synthesized and isolated. TpRu{P(OCH$_2$)$_3$CEt}(NCMe)Ph was found to initiate C−H activation of benzene and to catalyze the hydrophenylation of ethylene to produce ethylbenzene. Ethylene C−H activation to ultimately produce TpRu{P(OCH$_2$)$_3$CEt}(η^3-C$_3$H$_4$Me) kinetically competes with the catalytic hydrophenylation of ethylene. Computational studies were undertaken on reactions in the proposed catalytic ethylene hydrophenylation cycle as well as key side reactions.

Introduction

Transition metal systems have been demonstrated to activate the C−H bonds of a range of organic substrates.[1–3] The combination of metal-mediated C−H activation and C−C bond formation offers the potential for broad application and is an attractive target for catalytic C−H functionalization.[1,2,4–10] For example, the hydroarylation of olefins (Scheme 1) provides an atom-economical route to C−C bond formation with aromatic substrates that is complementary to established and useful catalytic cycles based on carbon-halide or carbon-triflate activation (e.g., Suzuki, Heck, Sonogashira, Stille, Negishi, and related reactions).[11–17] Although these catalysts have become important synthetic tools, such methodologies have limitations. For example, Suzuki and related reactions require the generation of carbon−halide bonds and typically produce stoichiometric metal waste. Lewis acid-catalyzed alkylation of aromatic substrates (i.e., Friedel−Crafts catalysis) has been both historically and practically important.[18] However, Friedel−Crafts catalysis often exhibits issues with selectivity (e.g., polyalkylation is a common problem) and in many cases consumes near-stoichiometric quantities of catalyst.[18] Advancements with new solid-state catalysts have provided improvements but require high temperatures, and polyalkylation remains problematic.[19]

Scheme 1. Hydrophenylation of Ethylene

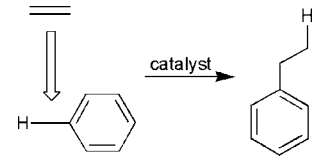

Progress has been made toward the development and understanding of single-site homogeneous catalysts for the hydroarylation of olefins;[1,2] however, catalysts that convert simple arenes (e.g., benzene) and unactivated olefins (e.g., ethylene, propylene, etc.) into alkyl arenes via metal-mediated C−H activation remain rare.[20–27] Our groups have been exploring the manipulation of a series of TpRu(L)(NCMe)Ar {L = CO, PMe$_3$, or P(pyr)$_3$; pyr = *N*-pyrrolyl; Ar = aryl} complexes that serve as homogeneous catalysts for the hydroarylation of olefins.[21,28–35]

* To whom correspondence should be addressed. E-mail: brent_gunnoe@ncsu.edu.
[†] North Carolina State University.
[‡] West Virginia University.
[§] University of North Texas.
[⊥] Sun Yat-sen University.

(1) Goj, L. A.; Gunnoe, T. B. *Curr. Org. Chem.* **2005**, *9*, 671–685.
(2) Ritleng, V.; Sirlin, C.; Pfeffer, M. *Chem. Rev.* **2002**, *102*, 1731–1769.
(3) Crabtree, R. H. *J. Chem. Soc., Dalton Trans.* **2001**, 2437–2450.
(4) Davies, J. A.; Watson, P. L.; Liebman, J. F.; Greenberg, A. *Selective Hydrocarbon Activation*; VCH: New York, 1990.
(5) Arndtsen, B. A.; Bergman, R. G.; Mobley, T. A.; Peterson, T. H. *Acc. Chem. Res.* **1995**, *28*, 154–162.
(6) Labinger, J. A.; Bercaw, J. E. *Nature* **2002**, *417*, 507–514.
(7) Goldman, A. S.; Goldberg, K. I. *Organometallic C-H Bond Activation*; American Chemical Society: Washington, D.C., 2004; Vol. 885, pp 1−43.
(8) Freund, M. S.; Labinger, J. A.; Lewis, N. S.; Bercaw, J. E. *J. Mol. Catal.* **1994**, *87* (1), L11−L15.
(9) Guari, Y.; Sabo-Etienne, S.; Chaudret, B. *Eur. J. Inorg. Chem.* **1999**, *7*, 1047–1055.
(10) Periana, R. A.; Bhalla, G.; Tenn, W. J.; Young, K. J. H.; Liu, X. Y.; Mironov, O.; Jones, C. J.; Ziatdinov, V. R. *J. Mol. Catal. A: Chem.* **2004**, *220*, 7–25.
(11) Beletskaya, I. P.; Cheprakov, A. V. *Chem. Rev.* **2000**, *100*, 3009–3066.
(12) Hassan, J.; Sévignon, M.; Gozzi, C.; Shulz, E.; Lemaire, M. *Chem. Rev.* **2002**, *102*, 1359–1469.
(13) Fanta, P. E. *Synthesis* **1974**, *1*, 9–21.
(14) Bolm, C.; Hildebrand, J. P.; Muniz, K.; Hermanns, N. *Angew. Chem., Int. Ed.* **2001**, *40*, 3284–3308.
(15) Stille, J. K. *Angew. Chem., Int. Ed. Engl.* **1986**, *25*, 508–524.
(16) Miyaura, N.; Suzuki, A. *Chem. Rev.* **1995**, *95*, 2457–2483.
(17) Heck, R. F. Vinyl Substitutions with Organopalladium Intermediates. In *Comparative Organic Syntheses*; Trost, B. M., Fleming, I., Semmelhack, M. F., Eds.; Pergamon Press: Oxford, 1999; Vol. 4, pp 833−863.
(18) Olah, G. A. ; Molnár, Á. *Hydrocarbon Chemistry*, 2nd ed.; Wiley-Interscience: New York, 2003; pp 229−232.
(19) Olah, G. A.; Molnár, Á. *Hydrocarbon Chemistry*, 2nd ed.; Wiley-Interscience: New York, 2003; pp 262−267.
(20) Matsumoto, T.; Taube, D. J.; Periana, R. A.; Taube, H.; Yoshida, H. *J. Am. Chem. Soc.* **2000**, *122*, 7414–7415.

10.1021/om800275b CCC: $40.75
Publication on Web 06/05/2008

Mechanistic studies implicate a catalytic cycle initiated by TpRu(L)(η^2-olefin)Ar formation via NCMe/olefin ligand exchange, olefin insertion into the Ru−Ph bond, aromatic coordination to the subsequent unsaturated Ru−alkyl complex, and aromatic C−H activation to release alkyl arene.[28] Initial studies of catalysis with TpRu(L)(NCMe)Ar systems that have compared the effects of altering the ancillary ligand "L" suggest that a ligand with significant π-acidity is optimal.[34,35] Consistent with this hypothesis, TpRu(CO)(NCMe)Ph is, to our knowledge, the most active homogeneous catalyst for the hydrophenylation of ethylene that proceeds through a metal-mediated C−H activation pathway.[21,28,29] However, this complex suffers from decomposition over a period of several hours under catalytic conditions. Studies of TpRu{P(pyr)$_3$}(NCMe)R (R = Me or Ph) have revealed that the steric profile of the P(pyr)$_3$ ligand, in combination with the bulky Tp ligand, acts to inhibit coordination of olefins, thus limiting catalysis.[35] In an effort to more precisely delineate the effects of the ancillary ligand "L" on Ru-mediated olefin hydroarylation activity, we sought to prepare and study the reactivity of TpRu{P(OCH$_2$)$_3$CEt}(NCMe)Ph. The bicyclic phosphite 4-ethyl-2,6,7-trioxa-1-phosphabicyclo-[2.2.2]octane, first prepared by Verkade et al.,[36,37] potentially offers a ligand with an amenable steric profile and a Ru system with metal-based electron density intermediate between that of the more electron-rich TpRu(PMe$_3$)(NCMe)R and the more electron-poor TpRu(CO)(NCMe)R systems. Herein, we disclose a combined experimental and computational study of ethylene hydrophenylation catalyzed by TpRu{P(OCH$_2$)$_3$CEt}(NCMe)-Ph.

Results and Discussion

Synthesis of TpRu{P(OCH$_2$)$_3$CEt}(NCMe)Ph. TpRu{P(OCH$_2$)$_3$CEt}(NCMe)Ph (**4**) was synthesized in four steps from the known complex TpRu(PPh$_3$)$_2$Cl (Scheme 2).[38] Refluxing TpRu(PPh$_3$)$_2$Cl in benzene with a slight excess of P(OCH$_2$)$_3$CEt for 3 h gives TpRu{P(OCH$_2$)$_3$CEt}(PPh$_3$)Cl (**1**) in 93% isolated yield. The ^{31}P NMR spectrum of complex **1** reveals two doublets (130.6 and 46.0 ppm) with $^2J_{PP}$ = 57 Hz. An X-ray diffraction study of a single crystal has confirmed the identity of **1** (Figure 1, Table 1). The structure of **1** reveals a pseudo-octahedral coordination sphere with the Ru−P(1) bond of PPh$_3$ {2.351(1) Å} elongated relative to the Ru−P(2) bond of P(OCH$_2$)$_3$CEt {2.202(1) Å}. A search of the Cambridge Structural Database

Scheme 2. Four-Step Synthesis of TpRu{P(OCH$_2$)$_3$CEt}(NCMe)Ph (4)

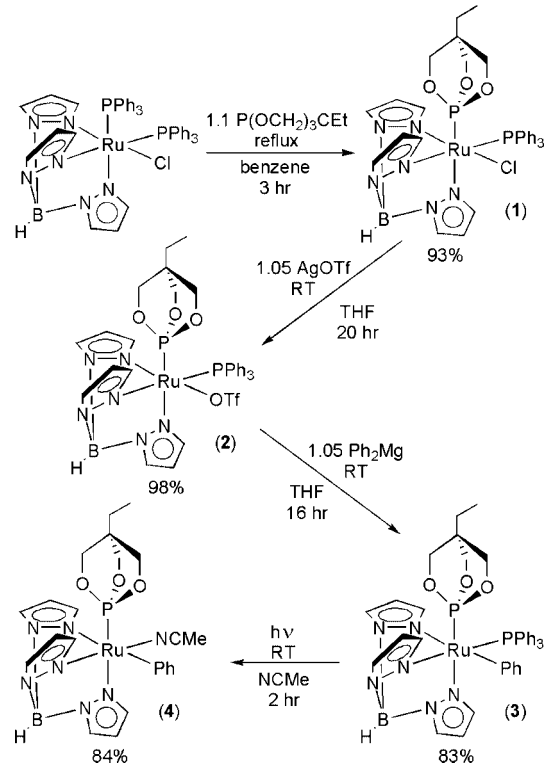

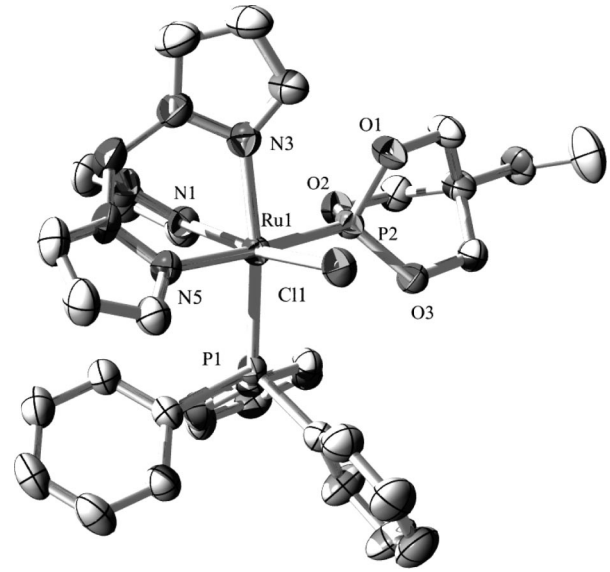

Figure 1. ORTEP of TpRu(PPh$_3$){P(OCH$_2$)$_3$CEt}Cl (**1**) (30% probability with hydrogen atoms omitted). Selected bond lengths (Å): Ru1−Cl1, 2.412(1); Ru1−P1, 2.351(1); Ru1−P2, 2.202(1); Ru1−N1, 2.092(3); Ru1−N3, 2.152(3); Ru1−N5, 2.139(3); P2−O1, 1.610(2); P2−O2, 1.611(2); P2−O3, 1.595(2). Selected bond angles (deg): P2−Ru1−P1, 94.71(3); P2−Ru1−Cl1, 87.45(3); P1−Ru1−Cl1, 97.67(3).

(21) Lail, M.; Arrowood, B. N.; Gunnoe, T. B. *J. Am. Chem. Soc.* **2003**, *125*, 7506–7507.
(22) Matsumoto, T.; Periana, R. A.; Taube, D. J.; Yoshida, H. *J. Mol. Catal. A.: Chem.* **2002**, *180*, 1–18.
(23) Periana, R. A.; Liu, X. Y.; Bhalla, G. *Chem. Commun.* **2002**, *24*, 3000–3001.
(24) Oxgaard, J.; Muller, R. P.; Goddard, W. A., III; Periana, R. A. *J. Am. Chem. Soc.* **2004**, *126*, 352–363.
(25) Oxgaard, J.; Periana, R. A.; Goddard, W. A., III *J. Am. Chem. Soc.* **2004**, *126*, 11658–11665.
(26) Karshtedt, D.; Bell, A. T.; Tilley, T. D. *Organometallics* **2004**, *23*, 4169–4171.
(27) Karshtedt, D.; McBee, J. L.; Bell, A. T.; Tilley, T. D. *Organometallics* **2006**, *25* (7), 1801–1811.
(28) Lail, M.; Bell, C. M.; Conner, D.; Cundari, T. R.; Gunnoe, T. B.; Petersen, J. L. *Organometallics* **2004**, *23*, 5007–5020.
(29) Pittard, K. A.; Lee, J. P.; Cundari, T. R.; Gunnoe, T. B.; Petersen, J. L. *Organometallics* **2004**, *23*, 5514–5523.
(30) Arrowood, B. N.; Lail, M.; Gunnoe, T. B.; Boyle, P. D. *Organometallics* **2003**, *22*, 4692–4698.
(31) Lail, M.; Gunnoe, T. B.; Barakat, K. A.; Cundari, T. R. *Organometallics* **2005**, *24*, 1301–1305.
(32) Pittard, K. A.; Cundari, T. R.; Gunnoe, T. B.; Day, C. S.; Petersen, J. L. *Organometallics* **2005**, *24*, 5015–5024.
(33) Goj, L. A.; Lail, M.; Pittard, K. A.; Riley, K. C.; Gunnoe, T. B.; Petersen, J. L. *Chem. Commun.* **2006**, *982*, 984.
(34) Foley, N. A.; Lail, M.; Lee, J. P.; Gunnoe, T. B.; Cundari, T. R.; Petersen, J. L. *J. Am. Chem. Soc.* **2007**, *129*, 6765–6781.
(35) Foley, N. A.; Lail, M.; Gunnoe, T. B.; Cundari, T. R.; Boyle, P. D.; Petersen, J. L. *Organometallics* **2007**, *26*, 5507–5516.
(36) Hutteman, T. J.; Foxman, B. M.; Sperati, C. R.; Verkade, J. G. *Inorg. Chem.* **1965**, *4*, 950.
(37) Verkade, J. G.; Reynolds, L. T. *J. Org. Chem.* **1960**, *25*, 663–665.
(38) Alcock, N. W.; Burns, I. D.; Claire, K. S.; Hill, A. F. *Inorg. Chem.* **1992**, *31*, 2906–2908.

Table 1. Selected Crystallographic Data for TpRu(PPh$_3$){P(OCH$_2$)$_3$CEt}Cl (1) and TpRu(PPh$_3$){P(OCH$_2$)$_3$CEt}OTf (2)

	complex **1**	complex **2**
empirical formula	$C_{33}H_{36}BClN_6O_3P_2Ru$	$C_{35}H_{38}BCl_2F_3N_6O_6P_2RuS$
fw	773.95	972.49
cryst syst	tetragonal	monoclinic
space group	$P4_12_12$	$P2_1/c$
a, Å	13.8513(5)	15.8186(8)
b, Å	13.8513(5)	14.9763(8)
c, Å	36.173(2)	18.0713(9)
β, deg		104.532(1)
V, Å^3	6940.0(5)	4144.2(4)
Z	8	4
D_{calcd}, g/cm^3	1.481	1.559
cryst size (mm)	0.26 × 0.36 × 0.48	0.26 × 0.40 × 0.68
R_1, wR_2 {$I > 2(I)$}	0.0324, 0.0765	0.0354, 0.1055
GOF	1.213	1.068

(CSD) produced fewer than 50 transition metal structures with coordinated P(OCH$_2$)$_3$CR (R = Me or Et) ligands and a single metal system bearing both a tris(pyrazolyl)borate and P(OCH$_2$)$_3$CR ligands, [Tp′W(CO){P(OCH$_2$)$_3$CEt}(η^2-MeC≡CMe)][BF$_4$] {Tp′ = hydridotris(3,5-dimethylpyrazolyl)borate}.[39] The most similar system to complex **1** that has been structurally characterized is Cp*Ru{P(OCH$_2$)$_3$CEt}$_2$Cl (Cp* = η^5-C$_5$Me$_5$), reported by Nolan et al., which has Ru−P bond distances {2.250(9) and 2.212(9) Å} comparable to complex **1**.[40]

Alkylation reactions that involve loss of chloride from TpRu−Cl systems are often unsuccessful. Thus, we sought a chloride/triflate metathesis to provide a more labile ligand. Complex **1** reacts with silver triflate at room temperature to form TpRu(PPh$_3$){P(OCH$_2$)$_3$CEt}OTf (**2**) (OTf = trifluoromethanesulfonate) in 98% isolated yield. The two resonances in the ^{31}P NMR spectrum of **2** (129.6 and 43.7 ppm, $^2J_{PP}$ = 56 Hz) shift slightly compared to complex **1**, and the ^{19}F NMR spectrum of **2** reveals a singlet at −76.2 ppm. Taken from a single-crystal X-ray diffraction study, Figure 2 (Table 1) shows a pseudo-octahedral geometry for complex **2** with the triflate ligand coordinated η^1 through an oxygen atom. The Ru−P bond lengths are similar to those of complex **1**, with the Ru−P(1) bond distance {2.364(1) Å} of the PPh$_3$ ligand of complex **2** elongated relative to the Ru−P(2) bond distance {2.212(1) Å} of the phosphite ligand. Comparing the Ru−N(1) bond length {2.092(3) Å} of the Tp arm trans to the Cl ligand for **1** reveals a trans effect, with the Ru−N bond 0.05 Å shorter than the average {2.146(4) Å} of the two other Ru−N bonds, which are trans to the P-donor ligands. The effect is enhanced in complex **2**, with the Ru−N(1) bond length {2.061(2) Å} of the pyrazolyl ring trans to the triflate ligand 0.08 Å shorter than the average Ru−N bond lengths {2.143(3} Å} trans to P-donor ligands.

Treating complex **2** with Ph$_2$Mg results in triflate/phenyl metathesis to form TpRu(PPh$_3$){P(OCH$_2$)$_3$CEt}Ph (**3**) in 83% isolated yield. Finally, the PPh$_3$ ligand of **3** can be exchanged for NCMe via photolysis in neat NCMe in approximately 2 h to give TpRu{P(OCH$_2$)$_3$CEt}(NCMe)Ph (**4**) as a white solid in 84% isolated yield. We have previously reported PPh$_3$/NCMe exchange under photolytic conditions for the synthesis of TpRu(PMe$_3$)(NCMe)Ph.[34]

Stoichiometric Benzene Activation. We have reported that TpRu(L)(NCMe)Me {L = CO, PMe$_3$, or P(pyr)$_3$} complexes initiate C−D bond activation of C$_6$D$_6$ at elevated temperatures to form TpRu(L)(NCMe)Ph-d_5 and CH$_3$D.[34,35] Likewise, TpRu(L)(NCMe)Ph (L = CO or PMe$_3$) systems activate C$_6$D$_6$ to release C$_6$H$_5$D and form TpRu(L)(NCMe)Ph-d_5.[34] Similarly, heating **4** in C$_6$D$_6$ results in the activation of a benzene-d_6 C−D bond to form TpRu{P(OCH$_2$)$_3$CEt}(NCMe)Ph-d_5 (**4-*d*$_5$**) and C$_6$H$_5$D (eq 1). Monitoring the activation of benzene-d_6 by **4** in neat C$_6$D$_6$ using ^{1}H NMR spectroscopy reveals the disappearance of the phenyl resonances at 7.75, 7.34, and 7.20 ppm along with approximately 25% decomposition to NMR-silent species (determined relative to an internal standard). For C$_6$D$_6$ activation by TpRu(CO)(NCMe)Ph, we have demonstrated that the addition of free NCMe suppresses decomposition to give quantitative conversion to TpRu(CO)(NCMe)Ph-d_5 along with reproducible kinetics,[34] and the addition of NCMe to the reaction between **4** and C$_6$D$_6$ also inhibits decomposition. For example, heating **4** at 60 °C in C$_6$D$_6$ with 1 equiv of NCMe (based on **4**) produces **4-*d*$_5$** and C$_6$H$_5$D with no evidence of decomposition versus an internal standard. Heating a triplicate set of **4** in C$_6$D$_6$ with 1 equiv of NCMe at 60 °C results in quantitative formation of TpRu{P(OCH$_2$)$_3$CEt}(NCMe)Ph-d_5 (**4-*d*$_5$**) with a k_{obs} of 1.20(2) × 10^{-5} s^{-1} taken from pseudo-first-order kinetic plots (see Figure 3 for a representative plot). In addition to the Ru-Ph/C$_6$D$_6$ exchange, ^{1}H NMR spectroscopy reveals H/D exchange

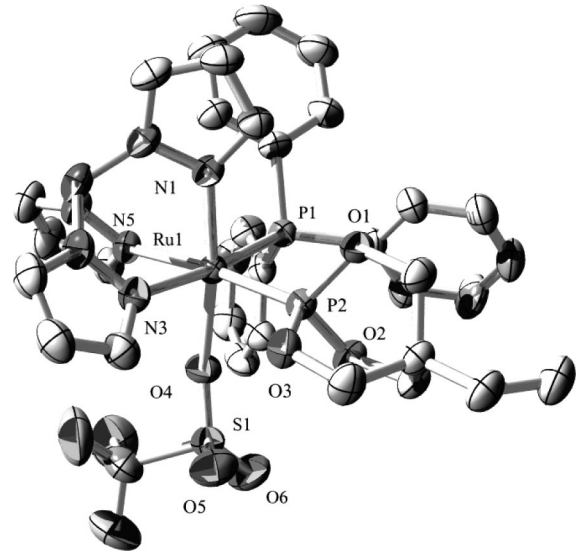

Figure 2. ORTEP of TpRu(PPh$_3$){P(OCH$_2$)$_3$CEt}OTf (**2**) (30% probability with hydrogen atoms omitted). Selected bond lengths (Å): Ru1−O4, 2.158(1); Ru1−P1, 2.364(1); Ru1−P2, 2.212(1); Ru1−N1, 2.061(2); Ru1−N3, 2.133(2); Ru1−N5, 2.153(2); P2−O1, 1.607(2); P2−O2, 1.597(2); P2−O3, 1.606(2); S1−O4, 1.457(2); S1−O5, 1.428(2); S1−O6, 1.427(2). Selected bond angles (deg): P2−Ru1−P1, 93.36(2); P2−Ru1−O4, 90.69(4); P1−Ru1−O4, 92.63(4); S1−O4−Ru1, 146.8(9).

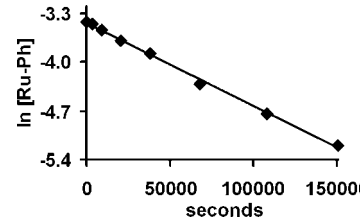

Figure 3. Representative pseudo-first-order plot of the rate of C$_6$D$_6$ activation by TpRu{P(OCH$_2$)$_3$CEt}(NCMe)Ph (**4**). Data were acquired by monitoring the disappearance of phenyl resonances of complex **4** by ^{1}H NMR spectroscopy.

(39) Adams, C. J.; Bartlett, I. M.; Boonyuen, S.; Connelly, N. G.; Harding, D. J.; Hayward, O. D.; McInnes, E. J. L.; Orpen, A. G.; Quayle, M. J.; Rieger, P. H. *Dalton Trans.* **2006**, 3466–3477.

(40) Serron, S. A.; Luo, L. B.; Stevens, E. D.; Nolan, S. P.; Jones, N. L.; Fagan, P. J. *Organometallics* **1996**, *15*, 5209–5215.

Scheme 3. Proposed Pathway for Benzene C−D(H) Activation by TpRu(L)(NCMe)Ph (L = CO, P{OCH$_2$}$_3$CEt, or PMe$_3$) {"□" indicates a vacant coordination site; [Ru] = TpRu(L)(NCMe)Ph}

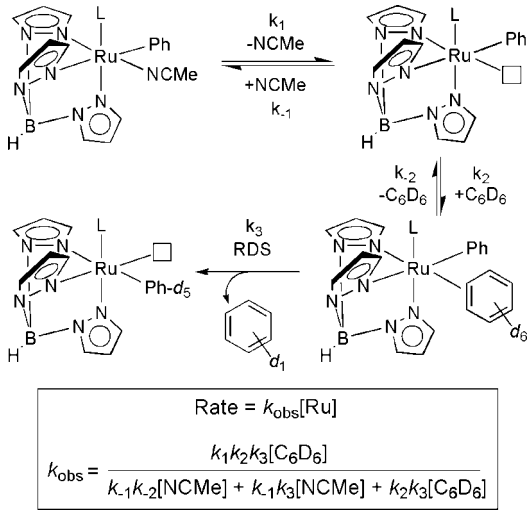

at the Tp 3/5 (22%) and Tp 4 (32%) pyrazolyl resonances. We have previously reported similar H/D exchange for TpRu(L)(L′)X systems where L = L′ = PMe$_3$ and X = OH, OPh, Ph, Me, or NHPh, or L = PMe$_3$, L′ = NCMe, and X = Ph.[41]

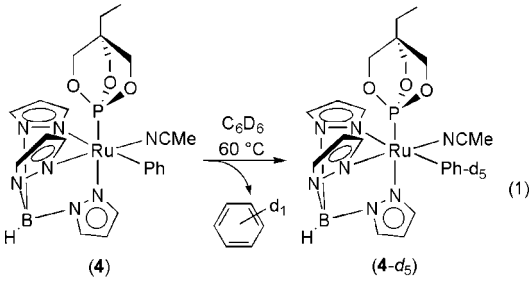

Mechanistic studies have indicated that C−H activation by TpRu(L)(NCMe)Ph (L = CO or PMe$_3$) systems likely proceeds by the pathway shown in Scheme 3.[28,29,34,42] Initial NCMe dissociation generates the unsaturated complex TpRu(L)Ph, and benzene coordination through either an η^1-C-H or η^2-C═C bond is followed by C−H activation to yield TpRu{P(OCH$_2$)$_3$CEt}-(NCMe)Ph-d_5 (**4-*d*$_5$**) upon coordination of NCMe. Kinetic studies, including intermolecular kinetic isotope effects for TpRu(L)(NCMe)Me (L = PMe$_3$ or CO), are consistent with this mechanism. For the C−H bond-breaking step, combined experimental and computational studies suggest a σ-bond metathesis type pathway with a Ru−H bonding interaction in the transition state (Chart 1).[25,28,43,44] Although computational modeling of the transition states was unable to locate *bona fide* Ru^{IV} oxidative addition intermediates,[45] the calculated close Ru−H contacts (<1.75 Å) in the C−H activation transition states suggest "oxidative character" in which Ru to H back-donation may play an important role in the transition-state energy. Such a reaction pathway has been labeled an oxidative hydrogen migration by Goddard, Periana, et al.[25,43]

Chart 1. Model of σ-Bond Metathesis Type Transition State for Benzene C−H Activation by TpRu(L)(R) {L = CO, PMe$_3$, or P(pyr)$_3$} Systems Based on Computational and Experimental Studies

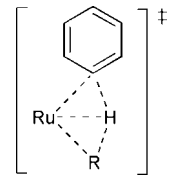

Table 2. Ru(III/II) Redox Potentials and Rate Constants for Benzene C−H(D) Activation by TpRu(L)(NCMe)Ph {L = PMe$_3$, P(OCH$_2$)$_3$CEt, P(pyr)$_3$, or CO}

L	Ru(III/II) (V)[a]	k_{obs} (10^{-5} s^{-1})[b]
PMe$_3$	0.29	1.36(4)
P(OCH$_2$)$_3$CEt	0.54	1.20(2)
P(pyr)$_3$	0.82	
CO	1.03	0.462(3)

[a] Versus NHE. [b] 60 °C in C_6D_6 with 1 equiv of NCMe.

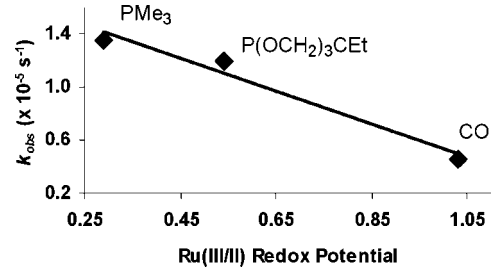

Figure 4. Plot of Ru(III/II) potentials (versus NHE) versus k_{obs} values for benzene (C_6D_6) C−D activation by TpRu(L)(NCMe)Ph {L = PMe$_3$, P(OCH$_2$)$_3$CEt, and CO} with R^2 = 0.97.

Given the evidence suggesting oxidative character in the benzene C−H activation transition state (see above), we have hypothesized that increasing the electron density on the Ru metal center might in turn increase the rate of aromatic C−H activation by TpRu(L)R systems.[34] Table 2 shows the rates of overall benzene C−H(D) activation and the Ru(III/II) potentials for the four TpRu(L)(NCMe)Ph complexes that we have studied {due to competitive decomposition, we were unable to determine a rate constant for the L = P(pyr)$_3$ system}. The Ru(III/II) potentials can be used to approximate the relative electron density of the four Ru metal centers. Despite the fact that there are a number of factors that contribute to the k_{obs} values for overall benzene C−H activation (see Scheme 3) as well as the Ru(III/II) potentials, a plot of k_{obs} versus Ru(III/II) potential gives a linear correlation with an R^2 of 0.97 (Figure 4). Although the data set is limited, this trend is consistent with the proposal that increased metal electron density facilitates the *overall* rate of benzene C−H activation, and the linear relationship suggests that d^6/d^5 redox potentials might be used as a predictor for the overall rate of aromatic C−H activation by TpRu(L)(NCMe)R catalysts and, potentially, for closely related d^6 complexes of Ru(II) and other transition metal systems.

Catalytic Hydrophenylation of Ethylene by TpRu-{P(OCH$_2$)$_3$CEt}(NCMe)Ph (4). Previously, we have reported that TpRu(L)(NCMe)Ph {L = CO, PMe$_3$, and P(pyr)$_3$} systems catalyze the hydrophenylation of ethylene.[21,34,35] Of the three systems, TpRu(CO)(NCMe)Ph was found to be the most active, yielding 55 TONs (turnover numbers) of ethylbenzene in 4 h

(41) Feng, Y.; Lail, M.; Foley, N. A.; Gunnoe, T. B.; Barakat, K. A.; Cundari, T. R.; Petersen, J. L. *J. Am. Chem. Soc.* **2006**, *128*, 7982–7994.
(42) Foley, N. A.; Gunnoe, T. B.; Cundari, T. R.; Boyle, P. D.; Petersen, J. L. *Angew. Chem., Int. Ed.* **2007**, *47*, 726–730.
(43) Oxgaard, J.; Goddard, W. A., III *J. Am. Chem. Soc.* **2004**, *126*, 442–443.
(44) DeYonker, N. J.; Foley, N. A.; Cundari, T. R.; Gunnoe, T. B.; Petersen, J. L. *Organometallics* **2007**, *26*, 6604–6611.
(45) Lail, M.; Bell, C. M.; Conner, D.; Cundari, T. R.; Gunnoe, T. B.; Petersen, J. L. *Organometallics* **2004**, *23*, 5007–5020.

Scheme 4. Proposed Pathway for Ethylene Hydroarylation by TpRu(L)(NCMe)Ph {L = CO, P(pyr)$_3$, P(OCH$_2$)$_3$CEt, or PMe$_3$} ("□" indicates a vacant coordination site)

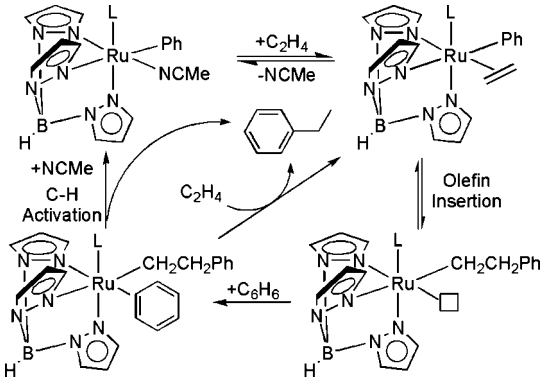

at 90 °C. Extensive investigations into the hydroarylation mechanism for all three systems suggest the catalytic pathway shown in Scheme 4.[28,29,34] Initiated by NCMe dissociation from TpRu(L)(NCMe)Ph, TpRu(L)Ph coordinates and mediates ethylene insertion into the Ru−Ph moiety. Benzene coordination and C−H activation produce ethylbenzene and regenerates the unsaturated TpRu(L)Ph complex to complete the catalytic cycle. The energetics of the two key steps, olefin insertion and benzene C−H activation, must be balanced for the catalytic pathway to proceed and avoid unwanted side reactions. For example, irreversible β-hydride elimination, irreversible C−H oxidative addition, olefinic C−H activation, and multiple insertions of olefin leading to oligomerization or polymerization of olefin can compete with the desired catalysis. Along these lines, studies of TpRu(L)(NCMe)R (L = CO, PMe$_3$, or P{pyr}$_3$; R = Me or Ph) complexes have allowed us to begin to delineate the electronic and steric parameters necessary for successful catalysis.[34,35] For example, kinetic isotope effects are consistent with the C−H activation event as the rate-determining step for ethylene hydrophenylation by TpRu(CO)(NCMe)Ph.[28] We have demonstrated that supplanting the CO ligand with PMe$_3$ increases the overall rate of benzene C−H activation (see above) by TpRu(L)(NCMe)Ph (L = CO or PMe$_3$);[34] however, the more electron-rich metal center of TpRu(PMe$_3$)(NCMe)Ph also serves to increase the overall activation barrier to olefin insertion, allowing for the emergence of a competitive ethylene C−H activation route that irreversibly shunts the active catalyst from the hydroarylation cycle.[34] Moving to the complex TpRu{P(pyr)$_3$}(NCMe)Ph provides a less electron-rich metal center than the TpRu(PMe$_3$)(NCMe)Ph system (Table 2). However, investigations with this system indicated that the steric bulk of the P(pyr)$_3$ ligand thwarted catalysis by preventing ethylene coordination.[35] The reduced cone angle (101°)[46] of the P(OCH$_2$)$_3$CEt ligand was anticipated to allow olefin coordination, while the moderate π-acidity of the phosphite was expected to potentially bias the kinetics toward olefin insertion over olefin C−H activation.

Heating TpRu{P(OCH$_2$)$_3$CEt}(NCMe)Ph (**4**) in benzene under ethylene pressure results in the catalytic production of ethylbenzene. Testing the reactivity from 10 to 1000 psi of ethylene and temperatures from 60 to 105 °C (note: 10 psi reactions were performed at 90 °C and below) revealed the optimal conditions for catalysis. Representative TONs after 28 h are shown in Figure 5. A maximum activity of approximately 10 TONs was achieved at 90 °C and 10 psi of ethylene. Catalytic trials carried out at 60 °C (not shown in Figure 5) gave less than 2 TONs after 28 h. Increasing the temperature to 105 °C results in an initial increase in the rate of ethylbenzene production, but overall nearly the same TONs after 28 h as reactions at lower temperatures. Figure 6 shows the general rates of catalysis for **4** in benzene at 25 psi of ethylene at 75, 90, and 105 °C. All reactions at these conditions yield a total of approximately 8 TONs of ethylbenzene. For reactions at temperatures greater than 90 °C, catalysis ceases after approximately 28 h of reaction. Increasing the pressure of ethylene decreased the overall production of ethylbenzene (Figure 5), suggesting that the rate of catalysis is inversely dependent upon olefin concentration. The same trend has been observed for catalytic olefin hydroarylation by TpRu(CO)(NCMe)Ph.[21,28]

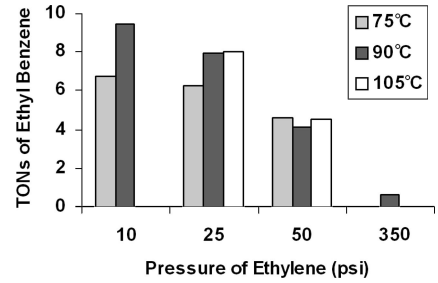

Figure 5. Select catalytic experiments for ethylene hydrophenylation using TpRu{P(OCH$_2$)$_3$CEt}(NCMe)Ph (**4**) at 75, 90, and 105 °C and 10, 25, 50, and 350 psi of C$_2$H$_4$. Ethylbenzene production is given in TONs relative to complex **4** after 28 h of reaction.

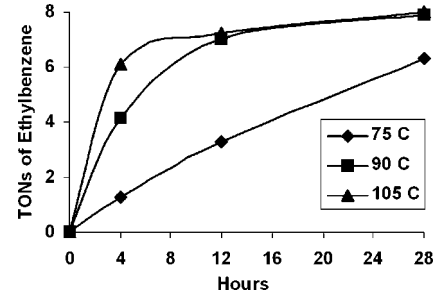

Figure 6. Comparison of catalytic hydrophenylation of ethylene by TpRu{P(OCH$_2$)$_3$CEt}(NCMe)Ph (**4**) at 75, 90, and 105 °C and 25 psi of C$_2$H$_4$. Ethylbenzene production is given in TONs relative to complex **4**. Continued monitoring of the reaction at 75 °C yielded a total of approximately 8 TONs after 51 h, at which time catalysis ceases.

Mechanistic investigations have indicated that ethylene C−H activation can compete with olefin hydroarylation for TpRu(L)(NCMe)Ph systems, and under certain conditions, this reaction is the predominant route for catalyst decomposition.[34] The initial ethylene C−H activation from TpRu(L)(η^2-C$_2$H$_4$)R (L= CO or PMe$_3$) ultimately leads to the formation of η^3-allyl complexes of the form TpRu(L)(η^3-C$_3$H$_4$Me). Scheme 5 illustrates the proposed pathway for ethylene C−H activation and allyl formation, based predominantly on ^{1}H NMR spectroscopy studies, in which ethylene C−H activation initially forms an unsaturated Ru−vinyl species and the coordination of a second equivalent of ethylene ultimately leads to the η^3-allyl complex.[34] Similar to TpRu(PMe$_3$)(NCMe)Ph, for complex **4**, recovery of the Ru system after catalysis reveals conversion to TpRu{P(OCH$_2$)$_3$CEt}(η^3-C$_3$H$_4$Me) (**5**) by ^{1}H NMR spectroscopy. Verification of the identity of complex **5** was obtained through independent synthesis by heating (70 °C) **4** in THF under 250 psi of C$_2$H$_4$ for 20 h (eq 2). Complex **5** was isolated in 67% yield and has been fully characterized. ^{1}H NMR spectroscopy reveals that the five resonances due to the allyl ligand of **5** are nearly coincident

(46) Tolman, C. A. *Chem. Rev.* **1977**, *77*, 313–348.

Scheme 5. Upon Dissociation of NCMe from TpRu(L)(NCMe)R {L = CO, $P(OCH_2)_3CEt$, or PMe_3; R = Me or Ph} and Coordination of Ethylene, Ethylene C−H Activation by TpRu(L)(η^2-C_2H_4)R Leads to the Formation of TpRu(L)(η^3-C_3H_4Me) ("□" indicates a vacant coordination site)

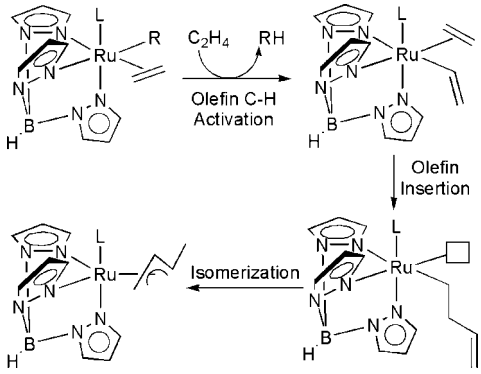

in chemical shift (δ) and coupling constants (J) to those for TpRu(CO)(η^3-C_3H_4Me) and TpRu(PMe_3)(η^3-C_3H_4Me).[34] Thus, for complex **4**, catalytic hydrophenylation of ethylene is observed, but C−H activation of ethylene ultimately competes with the rate of catalysis and serves to remove Ru from the catalytic cycle.

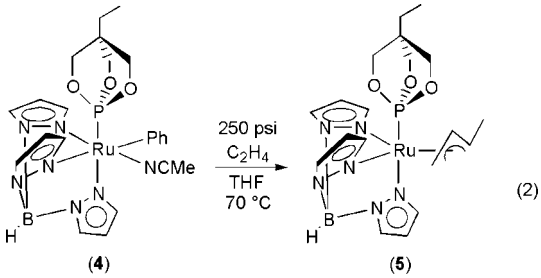

Computational Studies of Ethylene Hydrophenylation. A theoretical study of catalytic ethylene hydrophenylation and pertinent side reactions by TpRu{$P(OCH_2)CEt$}(NCMe)Ph was undertaken in order to provide additional insight. Computational studies (gas phase) were carried out using density functional and effective core potential methods {the B3LYP/CEP-31G(d) level of theory} at 298.15 K. The various reactions studied computationally are shown in Scheme 6.

Ethylene Hydrophenylation Catalytic Cycle. In accord with the overall catalytic cycle suggested in previous experimental and computational studies,[28,29,34] the energetics of all steps involved in the hydrophenylation of ethylene catalyzed by TpRu{$P(OCH_2)_3CEt$}(NCMe)Ph were calculated and are summarized in Scheme 7.

The first step in the catalytic cycle is dissociation of the NCMe ligand from the 18-electron catalyst precursor TpRu{$P(OCH_2)_3CEt$}(NCMe)Ph (**4**) to form a 16-electron active species TpRu{$P(OCH_2)_3CEt$}Ph, which is calculated to have an unfavorable ΔG of 16.1 kcal/mol. Ignoring the sterically bulky $P(pyr)_3$ system, a correlation of the binding energy of NCMe with the electronic impact of the ancillary "L" ligands of TpRu(L)(NCMe)Ph complexes is apparent. The TpRu(CO)(NCMe)Ph complex has the highest coordination energy of NCMe (17.3 kcal/mol), corresponding to the highest experimental Ru(III/II) potential (1.02 V versus NHE). The dissociation of NCMe from complex **4** is calculated to be less endergonic at 16.1 kcal/mol (versus the CO congener), while the dissociation of NCMe from TpRu(PMe_3)(NCMe)Ph is least endergonic (15.8 kcal/mol) among the three complexes. The experimental Ru(III/II) potentials (versus NHE) are 0.54 V for the $P(OCH_2)_3CEt$ complex **4** and 0.29 V for the PMe_3 complex.

Coordination of ethylene to the unsaturated species **B** leads to the η^2-C_2H_4 complex **C**. The process **B** + C_2H_4 → **C** is exergonic by 6.1 kcal/mol. We have previously reported that TpRu{$P(pyr)_3$}(NCMe)Ph does not coordinate ethylene, an experimental observation that is consistent with calculations that reveal the coordination of ethylene to the 16-electron system TpRu{$P(pyr)_3$}Ph is endergonic (by about 1 kcal/mol).[35] The contrasting affinity to coordinate ethylene for the phosphite system versus the $P(pyr)_3$ complex probably results from the prodigious steric effect of the bulky $P(pyr)_3$. The cone angle of the $P(pyr)_3$ ligand is 145°,[47] which is much larger than that of $P(OCH_2)_3CEt$ (101°). These calculated results are in accord with the experimental observations that the ethylene hydrophenylation catalyzed by TpRu(L)(NCMe)Ph occurs at low olefin pressure {between 10 and 25 psi for L = CO or $P(OCH_2)_3CEt$}, whereas ethylene hydrophenylation catalyzed by TpRu{$P(pyr)_3$}(NCMe)Ph occurs only at higher olefin pressure (>100 psi) and, even then, with minimal catalytic turnovers.[35]

The η^2-C_2H_4 complex **C** proceeds through a four-membered-ring transition state **TS1** for olefin insertion to form intermediate **D**, which possesses a κ^2-CH_2CH_2Ph ligand. The transition state **TS1** is similar to that of the insertion step in many olefin polymerization processes,[43] and the calculated $\Delta G^{\ddagger}$ for olefin insertion into the phenyl ligand of **C** is 19.9 kcal/mol. The calculated change in Gibbs free energy from the coordinatively unsaturated species **B** to **TS1** is only 13.8 kcal/mol, and starting from complex **4**, the change in Gibbs free energy to **TS1** is 29.9 kcal/mol.

The insertion step leads to an intermediate **D**, which is a β-phenethyl (Ru-CH_2CH_2Ph) complex. The most stable calculated conformer of intermediate **D** displays π-coordination of the phenyl to the ruthenium. Complex **D** is calculated to be 8.9 kcal/mol lower in energy than the 16-electron complex **B**, and the phenyl-to-Ru π-coordination in **D** likely serves to stabilize what would otherwise be an electronically unsaturated complex. The dihapto-coordination of benzene to **D** forms intermediate **E**. We have previously reported that TpRu(L)(C_6H_6)R complexes are calculated to have an interesting dichotomy in the benzene coordination mode (η^2-C═C vs η^2-C-H) due to the steric effects of co-ligand L, although the relative differences in free energies between them are very small.[34,35] The intermediate **E** with ligands PMe_3 and $P(pyr)_3$ are η^2-C-H (agostic) adducts, while **E** with the smaller ligand $P(OCH_2)_3CEt$ is calculated to have an η^2-C═C coordination style similar to that of the CO congener.

The benzene C−H activation step transforms **E** to yield the final products, ethylbenzene and active species **B**, through a σ-bond metathesis/oxidative hydrogen migration transition state **TS2**.[25,28,43,44] The calculated free energy of **TS2** is the highest species along the overall potential energy surface. Therefore, the calculations suggest that benzene C−H activation is the rate-determining step in the overall catalytic cycle using complex **4**. Experimental and computational studies of catalytic ethylene hydrophenylation catalyzed by TpRu(CO)(NCMe)Ph are consistent with benzene C−H activation as the rate-determining step.[28]

The calculated activation free energy (relative to **E**) for **TS2** is 37.4 kcal/mol (relative to **4**), lower than that for L = PMe_3 (40.1 kcal/mol),[34] but substantially higher than that for L = CO (30.9 kcal/mol).[34] As shown in Figure 7, a significant

(47) Moloy, K. G.; Petersen, J. L. *J. Am. Chem. Soc.* **1995**, *117*, 7696–7710.

Scheme 6. Depiction of the Catalytic Cycle for Ethylene Hydrophenylation and Competitive Side Reactions

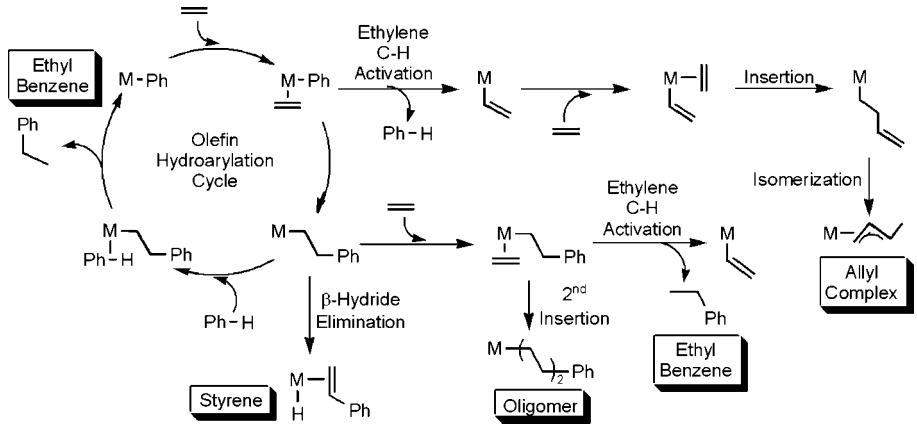

Scheme 7. Calculated Gibbs Free Energies (kcal/mol) for Steps in the Hydrophenylation of Ethylene Catalyzed by TpRu(L)(NCMe)Ph {L = $P(OCH_2)_3CEt$; "□" indicates a vacant coordination site; the transition state of dissociation of NCMe from complex 4 has not been calculated}

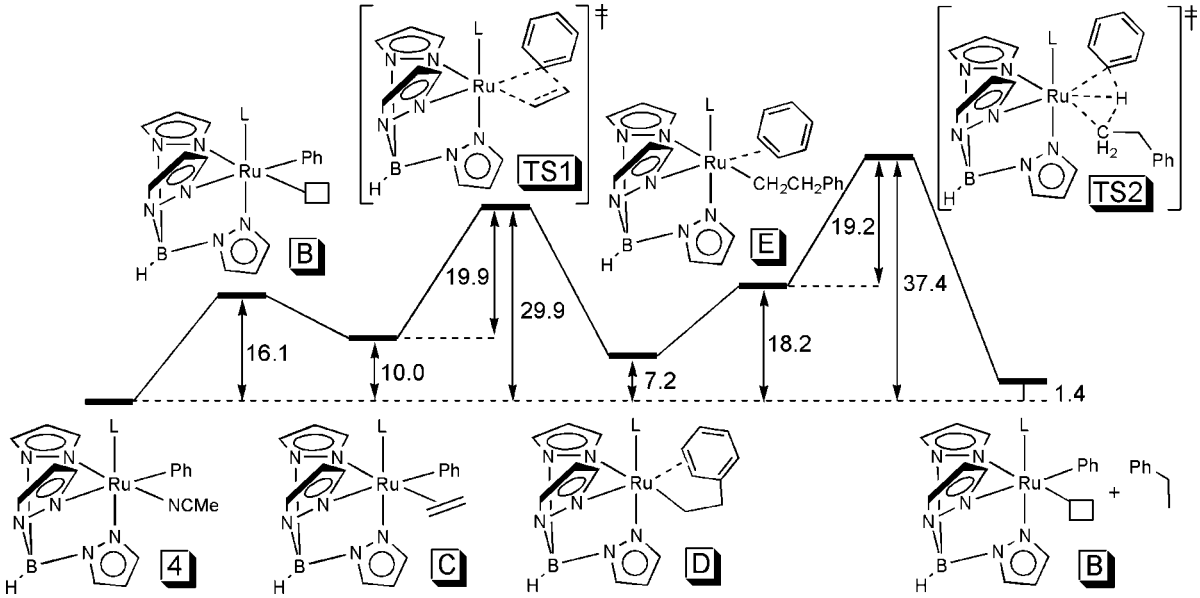

geometric difference in the three transition states is the orientation of the benzyl group of the phenethyl moiety. In the transition state for L = CO, the benzyl group is located proximal to the CO ligand. However, in transition states for L = $P(OCH_2)_3CEt$ and PMe_3, the benzyl groups rotate to a distal orientation relative to ligand L, a conformation likely due to steric repulsion from both L and Tp ligands. The $C_{CH2CH2Ph}\cdots H$ and $C_{Ph}\cdots H$ distances are different in magnitude for the different L ligands, Figure 7, but the relative position of these transition states along their respective reaction coordinates is similar, as suggested by $C_{CH2CH2Ph}\cdots H/C_{Ph}\cdots H$ ratios of ~1.03−1.05 for all three co-ligands. Interestingly, the L = CO TS, which has the most electronic-deficient metal center, also has the longest Ru···H distance among the three transition states

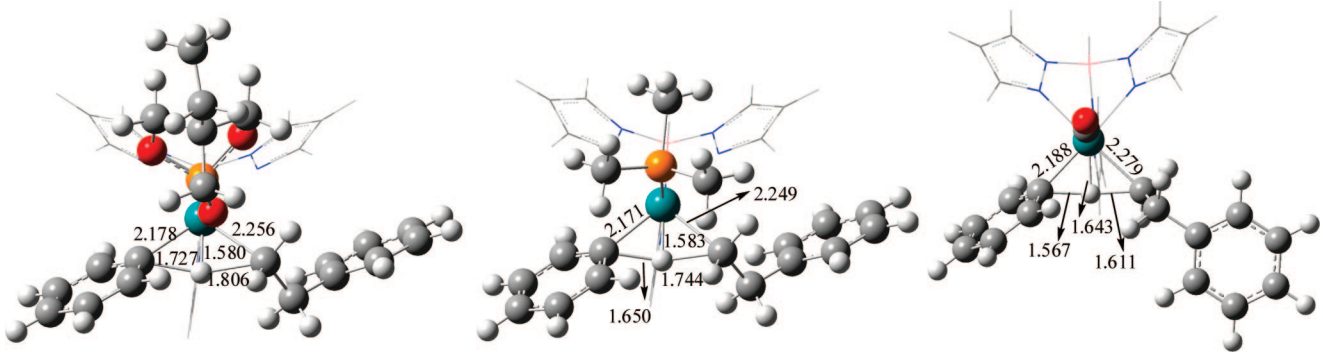

Figure 7. Comparison of calculated transition states for the benzene C−H activation step leading to ethylbenzene by TpRu(L)(benzene)CH_2CH_2Ph {L = $P(OCH_2)_3CEt$, shown on left; L = PMe_3, shown in middle; L = CO, shown on right}. The Tp ligands are shown in wireframe for clarity.

Scheme 8. Calculated Gibbs Free Energy (kcal/mol) for the Ethylene C−H Activation and Ethylene Insertion from TpRu(L)(η^2-C_2H_4)Ph {L = P(OCH$_2$)$_3$CEt}

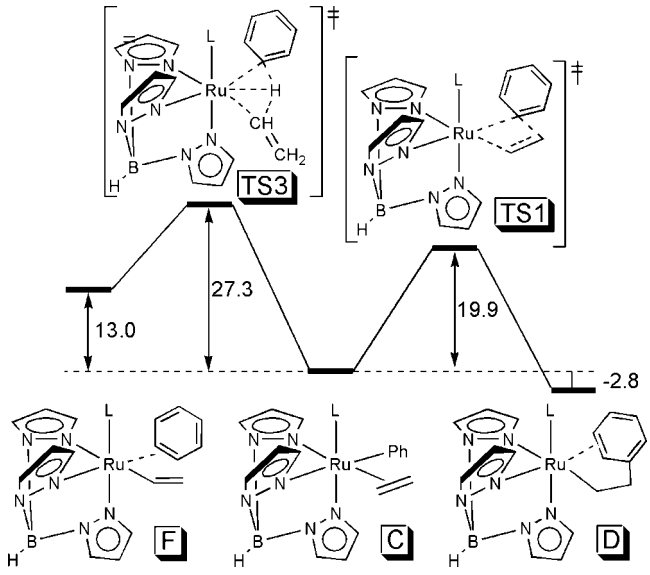

(1.64 Å versus 1.58 Å for the PMe_3- and phosphite-substituted transition states, Figure 7). The Ru−C bond distances in the TS for the CO complex are also elongated relative to the PMe_3 and P(OCH$_2$)$_3$CEt systems; however, the magnitude of the difference for the calculated Ru−C bond distances is less than for the relative Ru−H bond distances.

Olefin C−H Activation and Formation of TpRu{P(OCH$_2$)$_3$CEt}(η^3-C_3H_4Me) (5). As shown in Schemes 5 and 6, a primary side reaction that can compete with catalytic ethylene hydrophenylation is ethylene C−H activation to ultimately produce TpRu{P(OCH$_2$)$_3$CEt}(η^3-C_3H_4Me) (**5**). Similar to benzene C−H activation, ethylene C−H activation is calculated to proceed through a σ-bond metathesis/oxidative hydrogen migration transition state (**TS3** in Scheme 8) to form the Ru−vinyl intermediate **F**. Relative to the ethylene adduct **C**, the calculated activation free energy for the ethylene C−H activation step (27.3 kcal/mol) is considerably higher than that calculated for the ethylene insertion step (19.9 kcal/mol), which is consistent with the observation of several catalytic turnovers for ethylbenzene production before conversion to the allyl complex **5** (even if the calculated values do not coincide with experimentally determined relative rates). Ethylene C−H activation to give the Ru−vinyl complex **F** is calculated to be endergonic with ΔG = 13.0 kcal/mol, which, given the similar bond dissociation energies of benzene C−H bonds (∼110 kcal/mol)[48] and vinylic C−H bonds (∼111 kcal/mol),[48] likely reflects the difference in binding energies of η^2-ethylene (**C**) versus η^2-benzene (**F**). It might be anticipated that the intermediate **F** will easily revert to the η^2-C_2H_4 complex **C** through benzene C−H activation by the vinyl complex in a benzene solution with low ethylene concentration.

For catalytic hydrophenylation by TpRu(L)(NCMe)Ph where L = PMe_3 or P(OCH$_2$)$_3$CEt, we have experimental evidence that the formation of TpRu(L)(η^3-C_3H_4Me) complexes is the major pathway for catalyst decomposition. We have proposed that the allyl complexes are formed via an initial ethylene C−H activation step followed by an ethylene insertion and a consequent isomerization of the but-3-enyl ligand. as shown in Scheme 6. The potential energy surface for conversion of complex **4** to the allyl complex **5** was calculated (Scheme 9). As discussed above (see Scheme 8), intermediate **F** forms from ethylene C−H activation and can undergo benzene/ethylene exchange to form the thermodynamically more stable η^2-C_2H_4 complex **H**. The benzene/ethylene ligand exchange is calculated to be exergonic by approximately 16 kcal/mol. The ensuing ethylene insertion step involves a four-membered-ring transition state **TS4** with a calculated activation free energy of 17.4 kcal/mol (relative to **H**). This insertion leads to but-3-enyl complex **I**, which is calculated to possess a β-H agostic interaction with the C−H bond elongated to 1.2 Å (Figure 8, left). Subsequently, **I** can undergo a nearly barrier-free β-H elimination reaction (the calculated activation energy is 0.8 kcal/mol for **TS5** relative to **I**) to yield a hydride−butadiene complex **J1** with a ΔG of −9.2 kcal/mol. Rotation of the butadiene ligand in **J1** leads to isomer **J2**, which is 1 kcal/mol lower in free energy than **J1** (Figure 8, middle and right). The final allyl product **K** is proposed to form by hydrogen transfer from metal to butadiene through transition state **TS6**. This hydrogen transfer step is also calculated to be kinetically and thermodynamically feasible, with an activation free energy of 8.3 kcal/mol and a reaction free energy of −12.0 kcal/mol. Another possible hydrogen transfer pathway from the remote end of butadiene initiated directly from **J1** was also examined. The located transition state is shown in Scheme 9 as **TS7**. This transition state is calculated to have a substantially larger barrier of approximately 47 kcal/mol relative to **J1**.

We have disclosed a new olefin hydroarylation catalyst, TpRu{P(OCH$_2$)$_3$CEt}(NCMe)Ph (**4**), with reactivity that is consistent with our emerging picture of catalysis by TpRu(L)(NCMe)Ph systems. Complex **4** performs stoichiometric benzene C−H activation at a rate intermediate between the systems TpRu(L)(NCMe)Ph (L = CO and PMe_3), a trend that is likely reflective of the overall electron-donating ability of the ligand L. Additionally, relative to the reactivity studies of the previously reported TpRu{P(pyr)$_3$}(NCMe)Ph complex, catalysis with TpRu{P(OCH$_2$)$_3$CEt}(NCMe)Ph (**4**) highlights the importance for TpRu(L)R systems that the ligand L bear minimal steric imposition. The reactivity of complex **4** has been extended to ethylene hydrophenylation to yield moderate turnovers of ethylbenzene. Catalyst activity is ultimately halted by competitive ethylene C−H activation that leads to the irreversible formation of TpRu{P(OCH$_2$)$_3$CEt}(η^3-C_3H_4Me) (**5**). These results coupled with previous conclusions concerning the activity of TpRu(L)(NCMe)Ph {L = CO, P(pyr)$_3$, and PMe_3} systems help solidify a set of guidelines for viable hydroarylation catalysts of the form TpRu(L)(NCMe)R, in which the ligand L can be used to control the efficiency of substrate coordination *and* the rate of aromatic C−H activation, thus ultimately dictating the success for such systems to perform high yields of catalytic olefin hydroarylation. The ligand "L" must possess minimal steric bulk, and the d^6/d^5 redox potential should be near 1.0 V versus NHE. The impact of reduced electron density (i.e., more electron-deficient than TpRu(CO)(NCMe)R systems) has not yet been probed for this class of complexes. Such systems will likely require modification of the Tp ligand and are under analysis in our research laboratories.

Experimental Section

General Methods. Unless otherwise noted, all synthetic procedures were performed under anaerobic conditions in a nitrogen-filled glovebox or by using standard Schlenk techniques. Glovebox purity was maintained by periodic nitrogen purges and was monitored by an oxygen analyzer {O_2 < 15 ppm for all reactions}.

(48) Afeefy, Y.; Liebman, J. F.; Stein, S. E. Neutral Thermochemical Data. In *NIST Chemistry WebBook*, 2005.

Scheme 9. Calculated Gibbs Free Energies (kcal/mol) for the Formation of TpRu(L)(η^3-C_3H_4Me) (5) {L = $P(OCH_2)_3CEt$; "□" indicates a vacant coordination site}

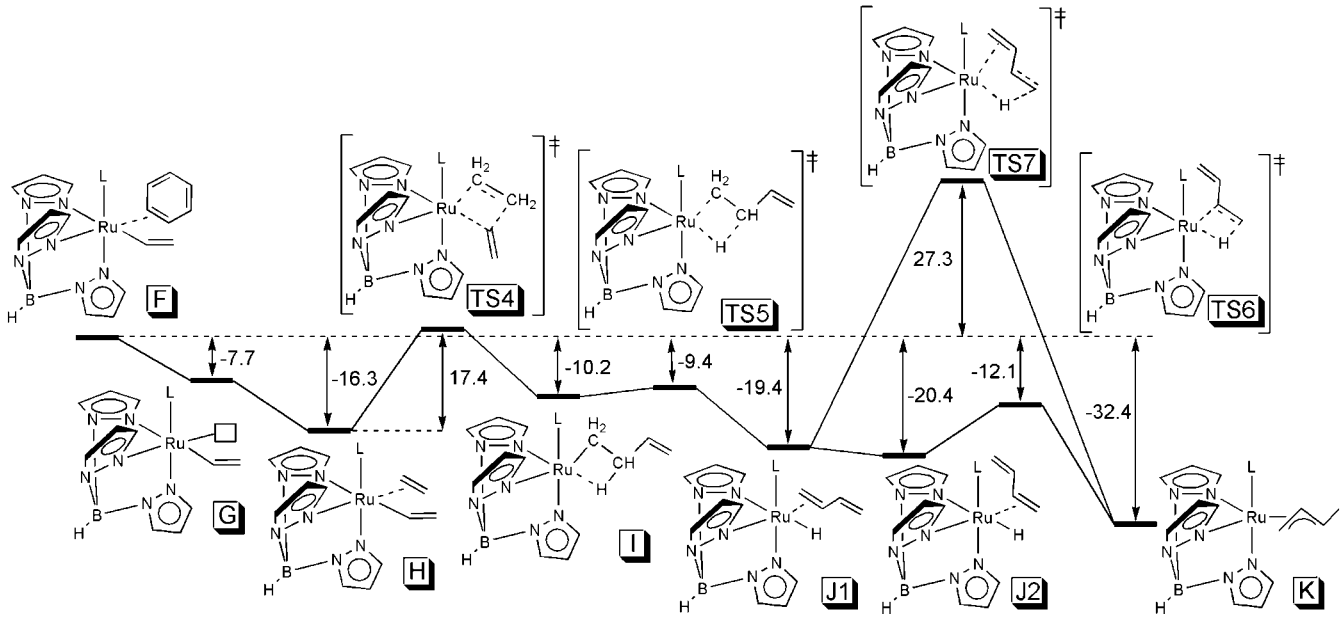

Benzene and tetrahydrofuran (stored over 4 Å molecular sieves) were dried by distillation from sodium/benzophenone. Pentane was distilled over sodium. Acetonitrile and methanol were dried by distillation from CaH_2. Hexanes were purified by passage through a column of activated alumina. Acetone-d_6, benzene-d_6, and chloroform-d_1 were degassed with three freeze−pump−thaw cycles and stored under a dinitrogen atmosphere over 4 Å molecular sieves. ^{1}H and ^{13}C NMR spectra were recorded on a Varian Mercury 300 or 400 MHz spectrometer. All ^{1}H and ^{13}C NMR spectra were referenced against residual proton signals (^{1}H NMR) or the ^{13}C resonances of the deuterated solvent (^{13}C NMR). ^{19}F NMR spectra were obtained on a Varian 300 MHz spectrometer and referenced against an external standard of hexafluorobenzene ($\delta = -164.9$ ppm). ^{31}P NMR spectra were obtained on a Varian 300 or 400 MHz spectrometer and referenced against an external standard of H_3PO_4 ($\delta = 0$). Resonances due to the Tp ligand are listed by chemical shift and multiplicity only (all coupling constants for the Tp ligand are approximately 2 Hz). Electrochemical experiments were performed under a nitrogen atmosphere using a BAS Epsilon potentiostat. Cyclic voltammograms were recorded in CH_3CN using a standard three-electrode cell from −2.00 to +2.00 V with a glassy carbon working electrode and tetrabutylammonium hexafluorophosphate as electrolyte. Tetrabutylammonium hexafluorophosphate was dried under dynamic vacuum at 110 °C for 48 h prior to use. All potentials are reported versus NHE (normal hydrogen electrode) using cobaltocenium hexafluorophosphate as the internal standard. GC-MS was performed using a HP GCD system with a 30 m × 0.25 mm HP-5 column with 0.25 mm film thickness. Ethylene (99.5%) was used as received from MWSC High-Purity Gases. $TpRu(PPh_3)_2Cl$,[38] $Ph_2Mg[THF]_2$,[49] and $P(OCH_2)_3CEt$[36] were prepared according to published procedures. All other reagents were used as purchased from commercial sources.

TpRu{P(OCH$_2$)$_3$CEt}(PPh$_3$)Cl (1). $TpRu(PPh_3)_2Cl$ (1.226 g, 1.403 mmol) and $P(OCH_2)_3CEt$ (0.250 g, 1.540 mmol) were heated to reflux in benzene (50 mL) for 3 h. The solvent was removed *in vacuo*, the residual material was dissolved in minimal THF, and a light yellow solid was precipitated with the addition of approximately 30 mL of hexanes. The precipitate was collected on a fine-porosity frit, washed with hexanes, and dried *in vacuo* (1.004 g, 1.628 mmol, 93%). X-ray quality crystals were grown by slow evaporation from a solution of **1** in CH_2Cl_2 layered with hexanes. ^{1}H NMR ($CDCl_3$, δ): 8.15, 7.64, 7.61, 7.51, 6.84, 6.73 (each 1H, each a d, Tp 3 or 5 positions), 7.37−7.15 (15 H, overlapping resonances, $P(C_6H_5)_3$), 6.08 (1H, m, Tp 4 position), 5.77, 5.73 (each 1H, each a m, Tp 4 positions), 4.05 {6H, d, $^3J_{HP} = 5$ Hz, $P(OCH_2)_3CEt$}, 1.13 {2H, q, $^3J_{HH} = 7.8$ Hz, $P(OCH_2)_3CCH_2CH_3$}, 0.76 {3H, t, $^3J_{HH} = 7.8$ Hz, $P(OCH_2)_3CCH_2CH_3$}. ^{13}C{^{1}H} NMR ($CDCl_3$, δ): 148.0, 145.2, 144.0, 136.2, 135.6, 134.5 (Tp 3 and 5 positions), 135.1 (d, $J_{CP} = 9$ Hz, ortho or meta of triphenylphosphine), 133.9 (d, $^1J_{CP} = 18$ Hz, ipso of triphenylphosphine), 128.9

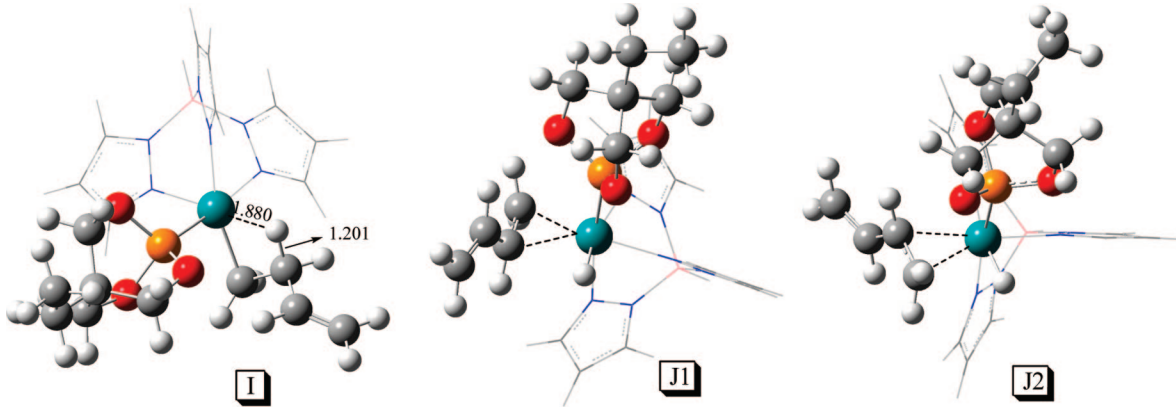

Figure 8. Optimized structures for intermediates **I**, **J1**, and **J2**. The Tp ligands are shown in wireframe for clarity.

(para of triphenylphosphine), 127.2 (d, J_{CP} = 9 Hz, ortho or meta of triphenylphosphine), 105.5, 105.1, 104.9 (Tp 4 positions), 73.9 {d, $^2J_{CP}$ = 7 Hz, P(O*C*H$_2$)$_3$CEt}, 35.0 {d, $^3J_{CP}$ = 31 Hz, P(OCH$_2$)$_3$*C*Et}, 23.7 {P(OCH$_2$)$_3$*C*CH$_2$CH$_3$}, 7.3 {P(OCH$_2$)$_3$CCH$_2$*C*H$_3$}. ^{31}P{^{1}H} NMR (CDCl$_3$, δ): 130.6 {d, $^2J_{PP}$ = 57 Hz, *P*(OCH$_2$)$_3$CEt}, 46.0 (d, $^2J_{PP}$ = 57 Hz, *P*Ph$_3$). EI-MS: *m*/*z* (%) $M_{theoretical}$ = 774.1160, M_{sample} = 774.1146 (σ = 2.8 ppm), [M$^+$].

TpRu{P(OCH$_2$)$_3$CEt}(PPh$_3$)OTf (2). To a solution of TpRu{P(OCH$_2$)$_3$CEt}(PPh$_3$)Cl (**1**) (0.442 g, 0.572 mmol) in THF (60 mL) was added AgOTf (0.154 g, 0.600 mmol). The mixture was stirred for 20 h at room temperature in a reaction vessel wrapped in aluminum foil. The yellow heterogeneous mixture was filtered through Celite on a fine-porosity frit. The volume of yellow filtrate was reduced under vacuum, a solid was precipitated with the addition of hexanes, and the light yellow solid was collected via vacuum filtration through a medium-porosity frit and dried *in vacuo* (0.496 g, 0.559 mmol, 98%). X-ray quality crystals were grown by slow evaporation from a solution of **2** in CH_2Cl_2 layered with hexanes. ^{1}H NMR (acetone-d_6, δ): 8.13, 8.05, 7.62, 6.80 (each 1H, each a d, Tp 3 or 5 positions), 7.93 (2H, overlapping resonances, Tp 3 or 5 positions), 7.49−7.15 (15 H, overlapping resonances, P(C$_6$*H*$_5$)$_3$), 6.27, 6.12, 6.09 (each 1H, each a m, Tp 4 positions), 4.20 {6H, m, *P*(OC*H*$_2$)$_3$CEt}, 1.26 {2H, q, $^3J_{HH}$ = 7.5 Hz, *P*(OCH$_2$)$_3$CC*H*$_2$CH$_3$}, 0.80 {3H, t, $^3J_{HH}$ = 7.5 Hz, *P*(OCH$_2$)$_3$CCH$_2$C*H*$_3$}. ^{13}C{^{1}H} NMR (acetone-d_6, δ): 150.7, 147.0, 144.3, 139.4, 137.4, 136.7 (Tp 3 and 5 positions), 135.5 (d, J_{CP} = 9 Hz, ortho or meta of triphenylphosphine), 133.9 (d, $^1J_{CP}$ = 43 Hz, ipso of triphenylphosphine), 131.0 (d, $^4J_{CP}$ = 2 Hz, para of triphenylphosphine), 128.9 (d, J_{CP} = 9 Hz, ortho or meta of triphenylphosphine), 122.6 (q, $^1J_{CF}$ = 322 Hz, Ru−O$_3$S*C*F$_3$), 107.6, 106.8, 106.7 (Tp 4 positions), 75.3 {d, $^2J_{CP}$ = 7 Hz, P(O*C*H$_2$)$_3$CEt}, 36.1 {d, $^3J_{CP}$ = 32 Hz, P(OCH$_2$)$_3$*C*Et}, 23.6 {P(OCH$_2$)$_3$*C*CH$_2$CH$_3$}, 7.3 {P(OCH$_2$)$_3$CCH$_2$*C*H$_3$}. ^{19}F{^{1}H} NMR (acetone-d_6, δ): −76.2 (C*F*$_3$). ^{31}P{^{1}H} NMR (acetone-d_6, δ): 129.6 {d, $^2J_{PP}$ = 56 Hz, *P*(OCH$_2$)$_3$CEt}, 43.7 (d, $^2J_{PP}$ = 56 Hz, *P*Ph$_3$). Anal. Calcd for C$_{34}$H$_{36}$BN$_6$P$_2$O$_6$SF$_3$Ru {NOTE: repeated efforts to dry this sample, including heating *in vacuo* after stirring/sonication in a variety of solvents (e.g., methylene chloride, pentane, and diethyl ether), did not remove residual solvent. Thus, 0.30 equiv of THF, 0.15 equiv of Et$_2$O, and 0.05 equiv of dichloromethane (observed and quantified by ^{1}H NMR spectroscopy) are included in elemental analysis calculations}: C, 46.57; H, 4.36; N, 9.09. Found: C, 46.61; H, 4.55; N, 8.74.

TpRu{P(OCH$_2$)$_3$CEt}(PPh$_3$)Ph (3). A solution of TpRu{P(OCH$_2$)$_3$CEt}(PPh$_3$)OTf (**2**) (0.477 g, 0.538 mmol) and Ph$_2$Mg[THF]$_2$ (0.182, 0.564 mmol) in THF (50 mL) was stirred at room temperature. After 16 h the THF was removed *in vacuo*, and the solid was dissolved in C$_6$H$_6$ (3 mL). The resultant mixture was filtered over a plug of silica, and a yellow filtrate was collected with successive THF washes. The filtrate was reduced *in vacuo* to ∼2 mL, and a light yellow solid was precipitated upon the addition of hexanes. The solid was collected over a fine-porosity frit, washed with pentane, and dried *in vacuo* (0.363 g, 0.446 mmol, 83%). ^{1}H NMR (C$_6$D$_6$, δ): 7.90 (1H, d, Tp 3 or 5 position), 7.65−7.60 (7H, overlapping resonances, Tp 3 or 5 positions and phenyl), 7.31−6.97 (18H, overlapping resonances, P(C$_6$*H*$_5$)$_3$ and phenyl), 6.04, 5.92, 5.64 (each 1H, each a m, Tp 4 positions), 3.38 {6H, m, P(OC*H*$_2$)$_3$CEt}, 0.12 {2H, q, $^3J_{HH}$ = 6.7 Hz, P(OCH$_2$)$_3$CC*H*$_2$CH$_3$}, 0.04 {3H, t, $^3J_{HH}$ = 6.7 Hz, P(OCH$_2$)$_3$CCH$_2$C*H*$_3$}. ^{13}C{^{1}H} NMR (C$_6$D$_6$, δ): 165.7 (dd, $^2J_{CP}$ = 19 Hz, $^2J_{CP}$ = 11 Hz, ipso of phenyl), 148.4 (phenyl), 147.8, 146.7, 146.6, 137.6, 137.1, 135.2 (Tp 3 and 5 positions), 135.4 (d, J_{CP} = 9 Hz, ortho or meta of triphenylphosphine), 134.6 (d, $^1J_{CP}$ = 19 Hz, ipso of triphenylphosphine), 127.7 (d, J_{CP} = 9 Hz, ortho or meta of triphenylphosphine), 125.3, 120.9 (phenyl resonances), 105.8, 105.0, 104.8 (Tp 4 positions), 73.4 {d, $^2J_{CP}$ = 8 Hz, P(O*C*H$_2$)$_3$CEt}, 34.1 {d, $^2J_{CP}$ = 31 Hz, P(OCH$_2$)$_3$*C*Et}, 23.5 {P(OCH$_2$)$_3$*C*CH$_2$CH$_3$}, 7.1 {P(OCH$_2$)$_3$CCH$_2$*C*H$_3$} {Note: the resonance due to the para positions of triphenylphosphine likely overlaps with the C$_6$D$_6$ resonance}. ^{31}P{^{1}H} NMR (C$_6$D$_6$, δ): 131.0 {d, $^2J_{PP}$ = 58 Hz, *P*(OCH$_2$)$_3$CEt}, 53.8 (d, $^2J_{PP}$ = 58 Hz, *P*Ph$_3$). Anal. Calcd for C$_{39}$H$_{41}$BN$_6$P$_2$O$_3$Ru {NOTE: repeated efforts to dry this sample, including heating *in vacuo* after stirring/sonication in a variety of solvents (e.g., methylene chloride, pentane, and diethyl ether), did not remove residual solvent. Thus, 0.11 equiv of THF and 0.14 equiv of hexanes (observed and quantified by ^{1}H NMR spectroscopy) are included in elemental analysis calculations}: C, 57.90; H, 5.29; N, 10.05. Found: C, 57.82; H, 5.36; N, 9.91.

TpRu{P(OCH$_2$)$_3$CEt}(NCMe)Ph (4). TpRu{P(OCH$_2$)$_3$CEt}(PPh$_3$)Ph (**3**) (0.128 g, 0.158 mmol) was added to acetonitrile (∼20 mL) in a thick-walled pressure tube with a Teflon stopper to give a light yellow solution. While stirring, the mixture was irradiated using a 450 W power supply (Ace Glass, Inc.) equipped with a water-cooled 450 W 5 in. arc IMMER UV−vis lamp (Ace Glass, Inc.) for a total of 2 h. The solvent was removed under reduced pressure, and the resulting solid was dissolved in 1 mL of THF. Hexanes (20 mL) were added to form a precipitate, which was collected on a fine-porosity frit and dried *in vacuo* (0.078 g, 0.132 mmol, 84%). ^{1}H NMR (C$_6$D$_6$, δ): 8.31, 8.07, 7.67 (each 1H, each a d, Tp 3 or 5 positions), 7.75 (2H, dd, $^3J_{HH}$ = 8.1 Hz and $^4J_{HH}$ = 1.5 Hz, ortho of phenyl), 7.60 (2H, overlapping Tp 3 or 5 positions), 7.36 (1H, Tp 3 or 5 position, partial overlap with phenyl), 7.34 (2H, t, $^3J_{HH}$ = 7.2 Hz, meta of phenyl), 7.20 (1H, tt, $^3J_{HH}$ = 7.2 Hz and $^4J_{HH}$ = 1.5 Hz, para of phenyl), 6.26 (1H, t, Tp 4 position), 6.04, 6.03 (each 2H, each a m, overlapping resonances, Tp 4 positions), 3.68 {6H, m, P(OC*H*$_2$)$_3$CEt}, 0.67 (3H, NCMe), 0.20 {2H, q, $^3J_{HH}$ = 7.5 Hz, P(OCH$_2$)$_3$CC*H*$_2$CH$_3$}, 0.03 {3H, t, $^3J_{HH}$ = 7.5 Hz, P(OCH$_2$)$_3$CCH$_2$C*H*$_3$}. ^{13}C{^{1}H} NMR (C$_6$D$_6$, δ): 170.8 (d, $^2J_{CP}$ = 19 Hz, ipso of phenyl), 147.5 (phenyl), 144.3, 143.4, 142.9, 135.5, 134.8, 134.2 (Tp 3 and 5 positions), 125.7, 120.6 (phenyl resonances), 120.1 (N*C*Me), 105.6, 105.5, 105.2 (Tp 4 positions), 73.5 {d, $^2J_{CP}$ = 8 Hz, P(O*C*H$_2$)$_3$CEt}, 34.7 {d, $^2J_{CP}$ = 30 Hz, P(OCH$_2$)$_3$*C*Et}, 23.6 {P(OCH$_2$)$_3$*C*CH$_2$CH$_3$}, 7.2 {P(OCH$_2$)$_3$CCH$_2$*C*H$_3$}, 2.9 (NC*C*H$_3$). ^{31}P{^{1}H} NMR (C$_6$D$_6$, δ): 132.8 {*P*(OCH$_2$)$_3$CEt}. Anal. Calcd for C$_{23}$H$_{29}$BN$_7$PO$_3$Ru {NOTE: repeated efforts to dry this sample, including heating *in vacuo* after stirring/sonication in a variety of solvents (e.g., methylene chloride, pentane, and diethyl ether), did not remove residual solvent. Thus, 0.04 equiv of Et$_2$O (observed and quantified by ^{1}H NMR spectroscopy) is included in elemental analysis calculations}: C, 46.57; H, 4.96; N, 16.41. Found: C, 47.12; H, 4.95; N, 16.39. CV (CH$_3$CN, TBAH, 100 mV/s): $E_{1/2}$ = 0.55 V {Ru(III/II), reversible}.

TpRu{P(OCH$_2$)$_3$CEt}(η^3-C$_3$H$_4$Me) (5). TpRu{P(OCH$_2$)$_3$CEt}(NCMe)Ph (**4**) (0.051 g, 0.087 mmol) was dissolved in THF (6 mL), sealed in a 15 mL stainless steel pressure reactor, pressurized to 250 psi with C$_2$H$_4$ and heated to 70 °C for 20 h. The volatiles were removed *in vacuo*, and the residue was dissolved in Et$_2$O (∼0.5 mL) and washed through a short plug of silica with a 1:1 mixture of Et$_2$O and hexanes. The resultant yellow filtrate was dried *in vacuo* (0.034 g, 0.058 mmol, 67%). ^{1}H NMR (C$_6$D$_6$, δ): 8.17, 8.08, 7.69, 7.64, 7.49, 6.87 (each 1H, each a d, Tp 3 or 5 position), 6.18, 6.11 (each 1H, each a t, Tp 4 position), 5.78 (1H, m, Tp 4 position), 4.84 (1H, m, "C"), 3.44 {6H, d, $^3J_{HP}$ = 4.8 Hz, P(OC*H*$_2$)$_3$CEt}, 2.99 (1H, dd, $^2J_{AB}$ < 1 Hz, $^3J_{AC}$ = 6.9 Hz, "A"), 2.32 (1H, dq, $^3J_{DC}$ = 11.0 Hz, $^3J_{DMe}$ = 5.5 Hz,, "D"), 2.01 (3H, d, $^3J_{MeD}$ = 5.7 Hz, Me), 1.39 (1H, dd, $^2J_{BA}$ < 1 Hz, $^3J_{BC}$ = 11.1 Hz, "B"), 0.12 {2H, q, $^3J_{HH}$ = 7.8 Hz, P(OCH$_2$)$_3$CC*H*$_2$CH$_3$}, −0.04 {3H, t, $^3J_{HH}$ = 6.9 Hz, P(OCH$_2$)$_3$CCH$_2$C*H*$_3$} {Note: see Chart 2 below for Ru-η^3-allyl proton labeling}. ^{13}C{^{1}H} NMR (C$_6$D$_6$, δ): 146.7, 144.5, 138.8, 135.2 (Tp 3 and 5 positions), 135.0 (2C, overlapping Tp 3 and 5 positions), 105.6 (Tp 4 position), 105.4 (2C, overlapping Tp 4 positions), 86.7, 53.4, 33.3 (allyl), 73.7 {d, $^2J_{CP}$ = 8 Hz, P(O*C*H$_2$)$_3$CEt}, 34.6 {d, $^2J_{CP}$ = 31 Hz, P(OCH$_2$)$_3$*C*Et},

(49) Lühder, K.; Nehls, D.; Madeja, K. *J. Prakt. Chem.* **1983**, *325*, 1027–1029.

Chart 2. Allyl Coupling Diagram for TpRu{P(OCH$_2$)$_3$CEt}(η^3-C$_3$H$_4$Me) (5)

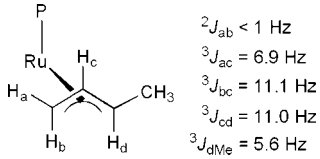

23.4 {P(OCH$_2$)$_3$*C*CH$_2$CH$_3$}, 19.4 (allyl methyl), 7.1 {P(OCH$_2$)$_3$CCH$_2$*C*H$_3$}. ^{31}P{^{1}H} NMR (CDCl$_3$, δ): 140.6 {*P*(OCH$_2$)$_3$CEt}. Anal. Calcd for $C_{19}H_{28}BN_6PO_3Ru$ {NOTE: repeated efforts to dry this sample, including heating *in vacuo* after stirring/sonication in a variety of solvents (e.g., methylene chloride, pentane, and diethyl ether), did not remove residual solvent. Thus, 0.17 equiv of hexanes (observed and quantified by ^{1}H NMR spectroscopy) is included in elemental analysis calculations}: C, 44.04; H, 5.61; N, 15.39. Found: C, 44.21; H, 5.57; N, 15.36.

Catalytic Hydroarylation Reactions. A representative catalytic reaction is described. TpRu{P(OCH$_2$)$_3$CEt}(NCMe)Ph (**4**) (0.013 g, 0.022 mmol) was dissolved in 2 mL of a stock solution of 0.1% hexamethylbenzene (HMB; internal standard) in benzene (0.145 g, 0.895 mmol of HMB in 80.0 mL of benzene). The homogeneous reaction mixture was placed in a stainless steel pressure reactor, charged with 50 psi ethylene pressure and heated to 90 °C. After 4, 12, and 28 h, the reaction was analyzed by GC-FID and the peak areas of the sample injection were used with the internal standard to calculate product yields. Ethylbenzene production was quantified using linear regression analysis of gas chromatograms. A set of five known standards were prepared consisting of 1:1, 2:1, 3:1, 4:1, and 5:1 molar ratios of ethylbenzene to hexamethylbenzene in benzene. A plot of the peak area ratios versus molar ratios gave a linear regression fit. The slope and correlation coefficient for ethylbenzene were 0.656 and 0.985, respectively.

Kinetic Studies: Rate Determination for Activation of C$_6$D$_6$ by TpRu{P(OCH$_2$)$_3$CEt}(NCMe)Ph (4). A solution of **4** (0.039 g, 0.065 mmol), 1 equiv of acetonitrile (3.4 μL, 0.07 mmol), and a small crystal of hexamethylbenzene as standard in 2 mL of C$_6$D$_6$ (22.6 mmol) was equally divided and transferred to three screw-cap NMR tubes. The set was heated to 60 °C in a temperature-regulated oil bath. ^{1}H NMR spectra were periodically acquired through 3 half-lives (using a pulse delay of 5 s). Relative to the internal standard hexamethylbenzene, the rates of Ru-Ph/Ru-Ph-d_5 exchange were followed by integration of the phenyl ortho resonance at 7.75. In addition, the rates of H/D exchange for the Tp 3/5 and the Tp 4 pyrazolyls were monitored by the resonances at 8.07 and 6.26 ppm, respectively.

Computational Methods. All calculations employed the Gaussian03 package.[50] The B3LYP functional (Becke's three-parameter hybrid functional[51] using the LYP correlation functional containing both local and nonlocal terms of Lee, Yang, and Parr)[52] and VWN (Slater local exchange functional[53] plus the local correlation functional of Vosko, Wilk, and Nusair)[54] were employed in conjunction with the Stevens (SBK) valence basis sets and effective core potentials for all heavy atoms and the -31G basis set for hydrogen. The SBK valence basis sets are valence triplet-ζ for ruthenium, and double-ζ for main group elements. The basis sets of main group elements are augmented with a d-polarization function: $\xi_d = 0.8$ for boron, carbon, nitrogen, and oxygen and $\xi_d = 0.55$ for phosphorus. The SBK scheme utilizes a semi-core (46-electron core) approximation for ruthenium and a full-core approximation for main group elements. All complexes modeled are closed-shell (diamagnetic) species and were modeled within the restricted Kohn−Sham formalism. All systems were fully optimized without symmetry constraint, and analytic calculations of the energy Hessian were performed to confirm species as minima or transition states and to obtain enthalpies and free energies (using unscaled vibrational frequencies) in the gas phase at 1 atm and 298.15 K.

Acknowledgment. We thank Dr. John G. Verkade of the Iowa State University Department of Chemistry for useful suggestions and a generous donation of the P(OCH$_2$)$_3$CEt ligand. T.B.G. acknowledges The Office of Basic Energy Sciences, United States Department of Energy (Grant No. DE-FG02-03ER15490), for support of this research. T.R.C. acknowledges the U.S. Department of Education for its support of the CASCaM facility. The research at UNT was supported in part by a grant from the Offices of Basic Energy Sciences, U.S. Department of Energy (Grants No. DEFG02-03ER15387). Calculations employed the UNT computational chemistry resource, which is supported by the NSF through grant CHE-0342824. T.R.C. also acknowledges the Chemical Computing Group for generously providing the MOE software. Z.K. acknowledges the State Scholarship Fund of CSC (No. 2007102840). Partial financial support for Z.K. was provided by the NSF-sponsored Center for Enabling New Technologies through Catalysis (CENTC; CHE-0650456).

Supporting Information Available: ^{1}H NMR spectra of complexes **1**, **2**, **3**, **4**, and **5** as well as complete tables of crystal data, collection and refinement data, atomic coordinates, bond distances and angles, anisotropic displacement coefficients for X-ray structures of complexes **1** and **2**. Cartesian coordinates for all calculated stationary points are also available. This material is available free of charge via the Internet at http://pubs.acs.org.

OM800275B

(50) Frisch, M. J.; Pople, J. A.;et al. *Gaussian03*; Gaussian Inc.
(51) Becke, A. D. *J. Chem. Phys.* **1993**, *98*, 1372–1377.
(52) Lee, C.; Yang, W.; Parr, R. G. *Phys. Rev. B* **1998**, *37*, 785–789.
(53) Kohn, W.; Sham, L. J. *Phys. Rev.* **1965**, *A140*, 1133.
(54) Vosko, S. H.; Wilk, L.; Nusair, M. *Can. J. Phys.* **1980**, *58*, 1200–1211.